

ARTICLES

State-to-State Vibrational Predissociation Dynamics of the Acetylene–HCl Complex

L. Oudejans and R. E. Miller*

Department of Chemistry, University of North Carolina, Chapel Hill, North Carolina 27599

Received: March 3, 1999; In Final Form: May 5, 1999

Photofragment translational spectroscopy has been implemented to obtain correlated final state distributions for the acetylene–HCl complex. Vibrational predissociation is induced by exciting the asymmetric acetylene C–H stretching vibration. In contrast with previous studies of this system, which suggested that the primary dissociation channel involves *intermolecular* V–V energy transfer (resulting in the production of $\nu = 1$ HCl), the present study shows that the dominant channel involves *intramolecular* V–V energy transfer, with the majority of the excess energy remaining with the acetylene subunit. In fact, the dissociation energy determined in the present study, $D_0 = 830 \pm 6 \text{ cm}^{-1}$, indicates that the HCl ($\nu = 1$) channel is closed.

Introduction

The literature on the vibrational predissociation of weakly bound complexes is extensive, with new developments having been made in both experiment^{1–3} and theory.^{4–10} For most of the systems that have been studied, the focus has been on the determination of the rate of dissociation, most often determined from measurements of the homogeneous line broadening observed in the spectrum,^{11–14} although real time measurements of the lifetime have also been carried out.¹⁵ From the wide range of systems that have been studied, some trends emerge that provide us with insights into the nature of the dissociation process. For example, it has long been recognized that energy or momentum gap considerations are important in these systems,^{10,16–19} the basic idea here being that the final states that tend to be favored are those with small translational recoil energies. The rationale for this is that there is poor overlap between the bound state wave function of the complex and continuum wave functions corresponding to high translational energies, the latter being highly oscillatory. Another trend indicates that the predissociation lifetimes decrease with increasing vibrational frequency shift (from the monomer to the complex).^{9,20} This clearly results from the fact that large frequency shifts are indicative of strong coupling between the intermolecular and intramolecular degrees of freedom, precisely the coupling needed for dissociation.

Armed with the lifetime–frequency shift correlation,^{9,20} one then considers with special care systems that deviate strongly from this behavior, presumably indicative of something more interesting. For example, excessive broadening in a spectrum has often been rationalized in terms of near resonances that make energy transfer and dissociation more facile.¹⁸ In the present study, we consider a case in point, namely, the acetylene–HCl complex. This system was first studied by microwave spectroscopy, which showed that it is T-shaped,²¹ with the HCl hydrogen bonded to the π cloud of the acetylene. In a previous infrared study,²² we showed that the line width resulting from

excitation of the asymmetric C–H stretching vibration was anomalously broad with respect to the frequency shift. When combined with the observation that the broadening of the acetylene–DCl complex was considerably smaller, we postulated that in the former case a near resonance might exist between the excited state of the complex (minus the dissociation energy) and the H–Cl fragment $\nu = 1$ vibrational state, enhancing the rate corresponding to the intermolecular V–V process. Subsequent pump–probe experiments by Rudich and Naaman²³ used REMPI spectroscopy to probe the $\nu = 1$ HCl fragment, following infrared pumping of the complex using an OPO laser. They indeed observed the production of $\nu = 1$ HCl in low rotational states, consistent with the near resonance picture, which implies that there is rather little excess energy available to the fragments. Unfortunately, this pump–probe method did not allow for the determination of the acetylene fragment states, nor the probing of the $\nu = 0$ HCl rotational states. Nevertheless, the combination of the spectroscopic and pump–probe studies seemed to provide rather conclusive evidence for intermolecular V–V energy transfer in this system.

In the current study, we have measured the photofragment angular distributions for acetylene–HCl using the optothermal method.²⁴ The acetylene–HCl complex is oriented in a strong electric field^{25–28} so that the photofragment angular distributions associated with the two monomer fragments can be recorded separately. This is possible because axial recoil of the oriented complex results in the two fragments recoiling in opposite directions in the laboratory frame. As shown below, the distributions observed here are inconsistent with the intermolecular V–V mechanism discussed above. Dissociation is found to proceed via the intramolecular V–V channel, resulting in the production of $\nu = 0$ HCl and acetylene in the C–C stretch excited state. At first, we thought that the disagreement with the previous results of Rudich and Naaman²³ was simply due to the fact that the intermolecular V–V process that produced HCl ($\nu = 1$) was only a minor channel, to which we were not sensitive in the present study, while the REMPI probe method was ideally suited to detect it. Nevertheless, as we will show

* Corresponding author. Fax: (919) 962-2388. E-mail: remiller@unc.edu.

herein, the dissociation energy we obtain from the present results indicates that the HCl ($v = 1$) channel is actually closed.

In addition to the previous experimental studies, there have been several ab initio calculations carried out for the acetylene–hydrogen chloride complex. In agreement with experiment, these studies give an equilibrium T-shaped structure for the complex. Unfortunately, the ab initio binding energies^{29–35} vary from 1.2 to 2.8 kcal/mol, depending on the method and basis set. Nevertheless, these results are still quite useful for comparison with the dissociation energy (D_0) obtained in the present study.

Experimental Method

The experimental apparatus used in the present study has been discussed in detail elsewhere.³⁶ It consists of a rotatable molecular beam source with two collimating skimmers to provide high angular resolution. An F-center laser intersects the molecular beam at the axis of rotation, where the complexes are excited and dissociate. In the present study, the F-center laser was operated on the RbCl:Li crystal (#3), pumped by 1.4 W from a krypton ion laser. This yielded approximately 30 mW of power in the region near 3300 cm^{-1} . Angular distributions were recorded for the particular initial state of the complex by varying the angle between the molecular beam and the line joining the photolysis volume and the bolometer detector, in 0.25° increments. Since the laser had to be held fixed on top of the transition of interest for a period of approximately 30 min, it was locked to an evacuated and temperature-stabilized confocal Etalon. Given that the transitions in the acetylene–HCl complex are quite broad,²² this presented no real problems. The short lifetime of the complex, in comparison with the flight time of the molecules to the detector, ensures that dissociation occurs within the laser excitation volume. Two electrodes flank the photolysis region for the purpose of applying a large dc electric field to the complexes so that they can be oriented prior to being excited by the laser. A bolometer detector is used to record the angular distributions for the two fragments, which recoil in opposite directions in the laboratory frame (the HCl recoiling toward the positive electrode and the acetylene toward the negative). Since the bolometer is an energy detector, the relative intensities of the two angular distributions provide us with information on the relative energy content of the two fragments. This form of photofragment microcalorimetry is the key to assigning the angular distributions discussed below to specific photofragment channels. To guarantee that the relative intensities of the two distributions are accurately determined, the intensities were compared at various angles by quickly reversing the polarity of the orienting electric field. This essentially eliminated the possible changes in intensities due to long-term fluctuations in laser power and bolometer sensitivity.

The complexes of interest were formed by expanding a 5% HCl and 6% acetylene in helium mixture through a 60 μm diameter room-temperature nozzle, from a source pressure of 500 kPa. The velocity of the parent complex, measured by Doppler spectroscopy³⁶ to be 1460 m/s, was needed to determine the recoil kinetic energy of the fragments from the laboratory scattering angle.

The rather large homogeneous line widths observed for the acetylene–HCl complex²² did not allow for the resolution of transitions associated with the ³⁵Cl and ³⁷Cl isotopic forms of the complex. Therefore, we will omit the use of the isotopic superscripts throughout the text and we simply assume that the dissociation dynamics of the two isotopic forms are the same. It is interesting to note that a similar study of the HF–H³⁵Cl and HF–H³⁷Cl photodissociation dynamics³⁷ showed that the

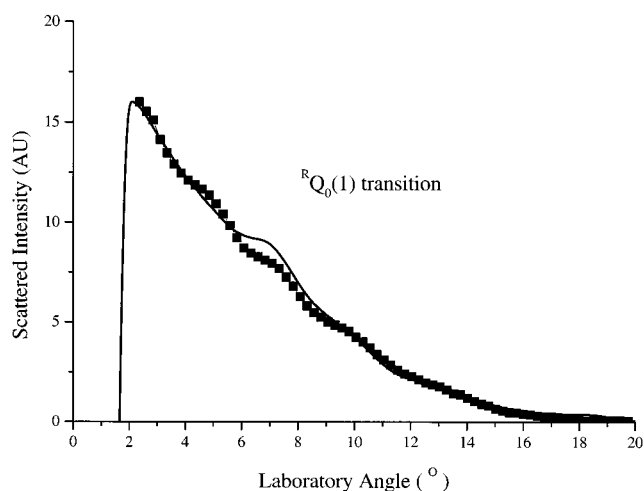


Figure 1. Experimental angular distribution for the acetylene–HCl complex following the excitation of the C–H stretch ${}^RQ_0(1)$ transition of the complex. The solid curve represents the calculated angular distribution for this transition using the probabilities obtained from the oriented angular distributions.

same set of open channels were indeed populated, although there were significant differences in the associated probabilities.

Results

In the preliminary stages of these experiments, we recorded photofragment angular distributions in the absence of an electric field. Since the complexes are not oriented in this case, the detector sees both fragments simultaneously. A typical angular distribution obtained in this way is shown in Figure 1, in this case pumping the ${}^RQ_0(1)$ transition of the complex. In this experiment, the laser polarization direction was aligned parallel to the molecular beam. The difficulty with data of this type is that it lacks the structure that we have used in the past³⁶ to determine the correlated final state distribution of the fragments. This is primarily due to the fact that the two fragments resulting from dissociation of this complex have very different masses and thus scatter to different laboratory angles. As a result, the angular distribution shown in Figure 1 is really a convolution of two distributions, one for each fragment, which results in significant blurring of the associated features. To overcome this difficulty, we made use of a strong dc electric field^{25–27} to orient the molecules so that the fragments recoil in opposite directions in the laboratory frame and thus can be detected separately.

The pendular state spectroscopy of the acetylene–HCl complex is complicated by the fact that the transition moment of the asymmetric C–H stretching vibration is perpendicular to the permanent electric dipole moment. The latter is largely accounted for by the vibrationally averaged projection of the HCl dipole moment on the A-axis of this T-shaped complex, while the transition moment is localized along the axis of the acetylene subunit. As a result, the A-axis of the complex becomes oriented with the electric field direction, which in the present experiments is arranged perpendicular to the molecular beam, in the detection plane. In the limit of perfect orientation, the acetylene axis will thus be perpendicular to the dc electric field. As a result, the optimum excitation occurs when the laser electric field is orthogonal to the dc field. A detailed discussion of the pendular spectroscopy and orientation distributions resulting from these conditions is given elsewhere, using the very similar case of acetylene–HF as an example.²⁸ As discussed therein, one observes a single intense transition in each of the K_a sub-bands associated with the perpendicular C–H

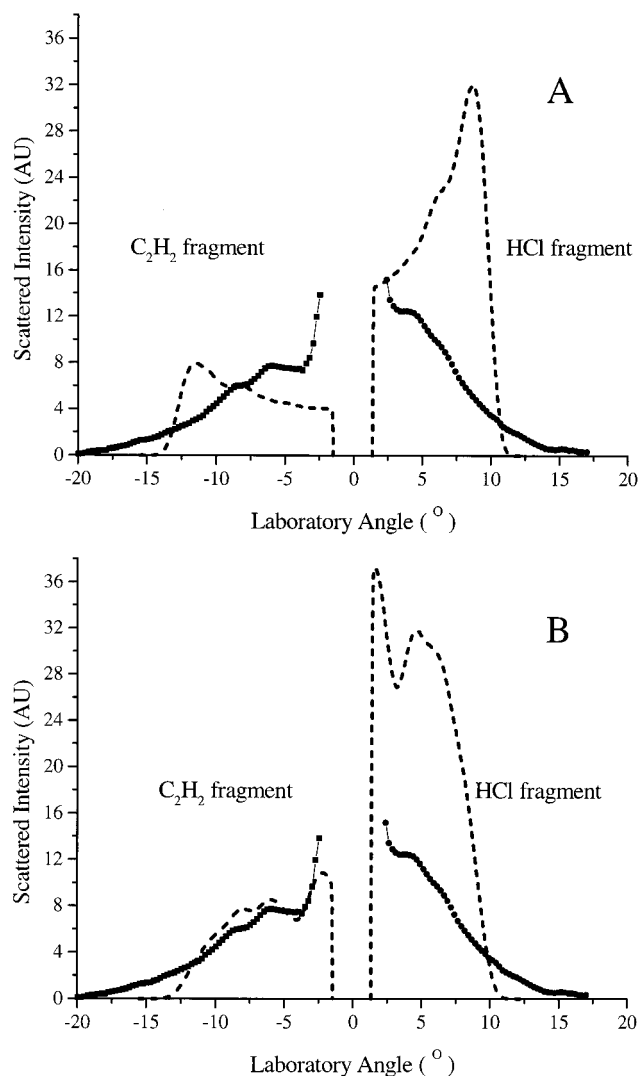


Figure 2. Comparison between the $K_a = 2 \leftarrow 1$ experimental angular distributions (data points) and those calculated based on the results of Rudich and Naaman²³ (dashed lines). The calculations shown in (A) and (B) correspond to two different acetylene rotational distributions and a dissociation energy (based on Rudich and Naaman) of 170 cm^{-1} .

stretching band of the complex, each one giving rise to a highly oriented excited state. For the present purposes, it is sufficient to say that the corresponding states are sufficiently oriented to ensure that the two fragments recoil in opposite directions in the laboratory frame of reference.

Angular distributions were obtained for pendular state transitions of the acetylene–HCl complex associated with the $K_a = 1 \leftarrow 0$, $K_a = 0 \leftarrow 1$, and $K_a = 2 \leftarrow 1$ sub-bands. An example of these data is given in Figure 2. The first thing to note is that there is now some structure in the experimental angular distributions, giving hope that we can obtain useful information on the final state distributions. Second, the position of the peaks on the two sides confirms that the parent complex is oriented, as shown by the fact that the heavier HCl fragment scatters to smaller angles than the lighter acetylene. At this point we should consider the factors that effect the relative intensities on the two sides. First, due to its smaller mass, the acetylene fragment recoils into a larger solid angle and as a result is less efficiently detected by the bolometer. As a result, if all else were equal, the signals associated with the acetylene fragment would be smaller than those for HCl. Another factor is the kinetic energy of the two fragments. Although conservation of momentum in the photodissociation process will result in more center-of-mass

recoil energy going into the lighter fragment, the laboratory frame kinetic energy is mainly determined by the stream velocity of the parent complex, which is clearly the same for both fragments. As a result, the laboratory frame kinetic energy is actually greater for the heavier fragment, namely HCl. Since the bolometer is an energy detector, this again favors the detection of HCl. There is also a difference in the sticking energy of the acetylene and HCl fragments to the bolometer, which is likely to be higher for the HCl fragment than for acetylene, due to hydrogen bonding. Thus, the combination of these three factors strongly favors the detection of the HCl fragment. Now if the HCl fragment was also produced in the $v = 1$ state, leaving the acetylene fragment with very little internal energy, the favoring of the HCl would be even more exaggerated. This is clearly at odds with the experimental results that show only a slight favoring of the HCl. The implication is that the acetylene fragment must carry away more internal energy than the HCl. This conclusion is surprising given the discussion of the previous work on this system^{22,23} that indicates that the primary dissociation channel involves a near resonant intermolecular V–V energy transfer, resulting in the vast majority of the excess energy appearing as HCl internal energy.

As noted above, Rudich and Naaman²³ have measured a final rotational state population distribution for HCl ($v = 1$), apparently produced from vibrational predissociation of the acetylene–HCl complex. Note that, for channels corresponding to the production of vibrationally excited HCl, only the vibrational ground state of acetylene is accessible. Since the acetylene rotational distributions were not measured in the study of Rudich and Naaman,²³ we must make some reasonable assumptions in order to calculate the expected angular distributions. In the analogous acetylene–HF complex,³⁸ we have found that acetylene rotational excitation is low and approximately Boltzmann, which is the initial assumption we also make here. In any case, the rotational constant of the acetylene is small enough that this degree of freedom cannot accommodate much energy.

The calculated angular distribution, based on the results of Rudich and Naaman,²³ which include all of the effects discussed above, is shown as the dashed curve in Figure 2A for the $K_a = 2 \leftarrow 1$ angular distribution. In this case, the rotational temperature of the acetylene fragment was fixed at 10 K for each of the four lowest ($v = 1$) HCl rotational states observed by Rudich and Naaman.²³ As expected, the signals on the HCl side of the angular distributions are much larger than on the acetylene side, since all of the detection factors now favor the HCl fragment. Clearly, this calculation not only gets the microcalorimetry wrong but also the shape of the individual angular distributions. Of course, the detailed shape of these angular distributions depends strongly on the rotational distributions of both fragments. Figure 2B shows the best fit to the experimental data (assuming the HCl is produced in $v = 1$ with the HCl fragment rotational distribution determined by Rudich and Naaman²³), obtained by varying the rotational distributions of the acetylene fragment, in this case yielding rotational (acetylene) temperatures of 15, 100, 150, and 300 K for the HCl rotational levels $j = 3, 2, 1$ and 0, respectively. Again, the signals on the HCl side remain much larger than those on the acetylene side, in contrast with the present experimental results.

We were completely unsuccessful in our attempts to reproduce the data assuming the HCl was produced in the $v = 1$ state. Not only is the microcalorimetry always wrong but the number and energies of the open rotational channels are completely inconsistent with the observed angular distributions.

For example, there is simply not enough available energy in this case to account for the observed scattering intensity at large angles, as indicated by the sharp cutoff of the calculated distributions. It is important to note that the comparison between the calculated distributions based on the Rudich and Naaman results²³ and the present experimental results assumes that the initial excitation of the complex is the same in both experiments. Although Rudich and Naaman point out that their temperature is higher than that in our previous study²² (which is the same as in the present study), we will show below that the K_a dependence of the photofragment angular distributions is insufficient to account for the differences.

In the previous study of the acetylene–HF complex,³⁸ we proceeded to assign the final states by probing the fragments with a second F-center laser. Unfortunately, the signal levels were considerably lower in the present experiments, mainly due to the large lifetime broadening of the complex. As a result, the probe laser experiments were not possible in this case. Nevertheless, the fact that excitation of the same acetylene mode in acetylene–HF³⁸ leads to the production of the acetylene fragment in the C–C stretching excited state may be taken as a first indication of what might be going on here.

Rudich and Naaman²³ concluded, from the observation of the HCl in $\nu = 1$, that the dissociation energy of this complex was between 170 and 260 cm^{-1} . Unfortunately, we were unsuccessful in fitting the experimental angular distributions using dissociation energies in this range, even when allowing for the production of the acetylene fragment in the C–C stretch excited state, the problem being that the resulting available energy for rotation was approximately 1000 cm^{-1} , presumably mainly in the HCl fragment. At this level of rotational excitation, the density of HCl rotational states is too sparse to account for the experimental angular distributions. Therefore, we were forced to conclude that the dissociation energy obtained by Rudich and Naaman²³ is too small.

We are now left with the task of determining the dissociation energy of the acetylene–HCl complex directly from the photofragment angular distributions. If we assume that all possible vibrational and rotational channels are feasible and that any combination of these states represents a feasible distribution, we would be unable to obtain a unique assignment of the angular distribution without the aid of the pump–probe experiments, due to the high density of fragment channels. As a result, we must restrict the channels we include in the analysis. As noted above, we have the acetylene–HF results to guide us, suggesting that the C–C stretching mode of the acetylene fragment is the receptacle of most of the available energy.³⁸ Fortunately, we have support for this assignment from the angular distributions obtained here in the form of the relative intensities. Indeed, if we assume that the acetylene fragment is produced in the C–C stretch excited state and the HCl takes away most of the remaining energy as rotation, the calculated angular distributions have the correct relative intensities. It is important to note that there are other nearby vibrational levels that are also consistent with the microcalorimetry; however, these are combination bands that are expected to be relatively weakly coupled to the excited state of the complex. Given all of this evidence, we proceeded to analyze the data based on the acetylene fragment being produced exclusively in the C–C stretch excited state.

On the basis of the above vibrational assignment, we carried out an extensive search for possible dissociation energies, with the result being that only a single value ($D_0 = 830 \pm 6 \text{ cm}^{-1}$) gave good fits to all three angular distribution sets. We note here that the error bar for the dissociation energy is somewhat

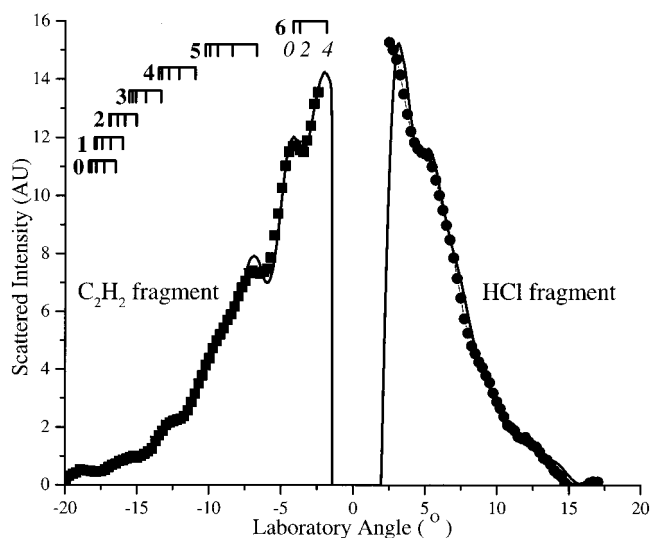


Figure 3. Photofragment angular distributions for oriented C_2H_2 –HCl, pumping the $K_a = 1 \leftarrow 0$ sub-band of the asymmetric C–H stretch. The solid line through the data points represents the best fit obtained using a Monte Carlo procedure to include the instrumental factors that control the resolution. The free parameters in the fit are the relative probabilities for producing the various (correlated) $j(\text{HCl})$, $j(\text{C}_2\text{H}_2)$ fragment states. The acetylene fragment is taken to be in the C–C stretch excited state, based on the microcalorimetry. The peak positions of the individual channels are indicated by bars above the acetylene side of the angular distribution. The numbers 0 through 6 correspond to j of the HCl, and the even numbers under the bar correspond to the rotational states of the acetylene fragment.

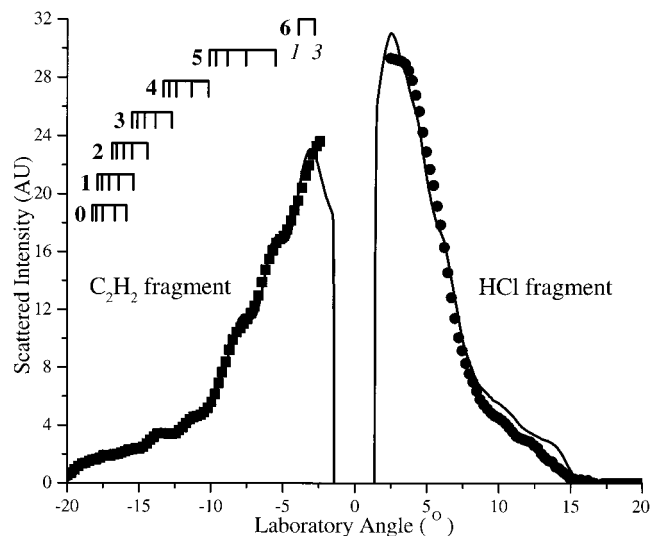


Figure 4. Photofragment angular distributions of oriented C_2H_2 –HCl, pumping the $K_a = 0 \leftarrow 1$ sub-band of the asymmetric C–H stretch. In this case, only the odd acetylene j states are included, as discussed in the text.

larger than some of the other systems we have studied, due to the fact that not all of the acetylene rotational structure is resolved in the angular distributions. The solid lines through the data in Figures 3, 4, and 5 show the resulting fits, corresponding to excitation of the pendular features in the $K_a = 1 \leftarrow 0$, $K_a = 0 \leftarrow 1$, and $K_a = 2 \leftarrow 1$ sub-bands, respectively. Clearly, this assignment gets the microcalorimetry correct for all three K_a' angular distributions and reproduces all of the fine structure in the angular distributions. These fits were obtained by adding the additional constraint that the acetylene fragment populates only low j states, consistent with the previous acetylene–HF study.³⁸ In the absence of this constraint, other

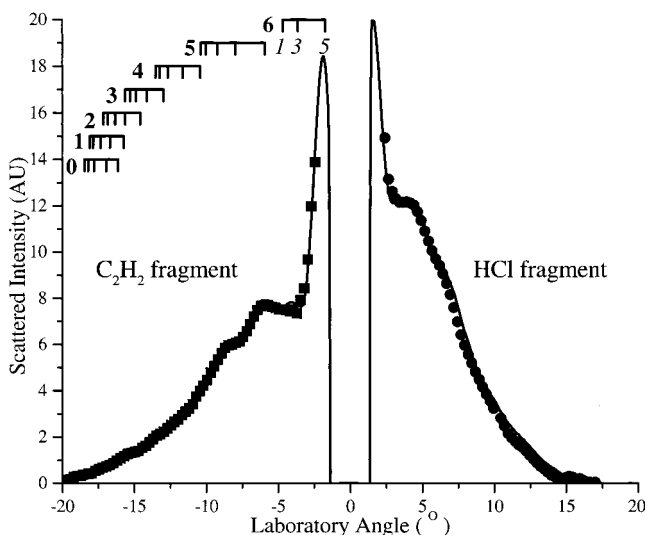


Figure 5. Photofragment angular distributions of oriented C_2H_2 -HCl, pumping the $K = 2 \leftarrow 1$ sub-band of the asymmetric C-H stretch. Once again, only the odd acetylene j states are included in the fit.

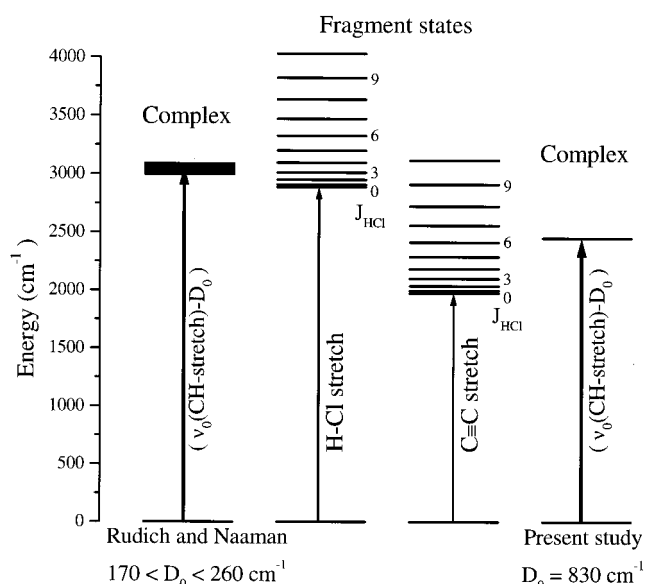


Figure 6. Photofragment energy level diagram for the photodissociation of C_2H_2 -HCl. Each HCl rotational state is built upon the available vibrational state of the C_2H_2 and HCl fragment. The vertical arrow on the left indicates the available energy (to the fragments) based upon the D_0 determined from the previous study (170 cm^{-1}),²³ while the arrow on the right indicates the available energy based on the dissociation energy as obtained in this study (830 cm^{-1}).

solutions with significantly different dissociation energies were found. Nevertheless, the resulting acetylene rotational distributions were erratic in these cases and did not give results that were at all consistent with the acetylene-HF system³⁸ or indeed any of the results we have obtained for other systems.^{39–41} We therefore feel that the present assignment is compelling.

The energy level diagram in Figure 6 shows a comparison between all of the photofragment channels discussed above. As noted previously, the translational/rotational energy available to the fragments is considerably larger for the C-C stretch channel compared with HCl ($\nu = 1$). As a result, this channel also properly reproduces the larger angle portion of the angular distributions. It should be emphasized that we can rule out the production of significant quantities of ground vibrational state acetylene from the microcalorimetry. Ground vibrational state acetylene could only be produced in coincidence with vibra-

tionally or highly rotationally excited HCl, which we have already shown to be inconsistent with the data.

It is also important to point out that in the above analysis we have included only even (odd) j rotational states for the acetylene fragment when pumping the odd (even) K_a states of the complex. Since K_a rotation of the complex correlates with j of the acetylene fragment and the nuclear spins are conserved in the dissociation process, even and odd K_a states will dissociate into a different set of acetylene rotational states. Since the asymmetric C-H vibrationally excited state of the complex is ungerade, dissociation into acetylene vibrational states of the same symmetry as the vibrational ground state (Σ_g^+) from even (odd) K_a states of the complex will result in the population of odd (even) j states of the acetylene fragments. The vibrational state of importance in the present case is the C-C stretch, which is indeed of Σ_g^+ symmetry.

Discussion

The data discussed above show rather convincingly that the primary dissociation channel for acetylene-HCl, excited to the asymmetric C-H stretch excited state, involves intramolecular V-V energy transfer to the C-C stretch excited state, as has been observed previously for acetylene-HF.³⁸ The fits to the present data yield a dissociation energy of $830 \pm 6 \text{ cm}^{-1}$, indicating that the $\nu = 1$ HCl channel is closed. This leaves us to speculate concerning the source of the $\nu = 1$ HCl in the study of Rudich and Naaman.²³ One possibility is that larger clusters were present in the previous study and were excited by the relatively lower resolution of the pump laser. These larger clusters could certainly have very different photodissociation dynamics, possibly leading to the production of $\nu = 1$ HCl. It is important to note that in the study of Rudich and Naaman a detailed assignment of the infrared spectrum of the complex was not given. Alternatively, since this study was carried out in a molecular jet, where some collisions may still be occurring, it is possible that the HCl ($\nu = 1$) was produced by collisional V-V transfer from acetylene, rather than from photofragmentation. Rudich and Naaman²³ observed a Boltzmann distribution for the HCl fragment, which is something we generally do not see in the dissociation of complexes. Instead, we normally observe strongly inverted rotational distributions with the HX fragment produced preferentially in the highest open j state. This may also be an indication that the distribution observed by Rudich and Naaman comes from some other process.

As discussed above, the angular distributions are dependent upon the K_a state that is pumped. The vertical bars in Figures 3–5 represent the peak positions of the open channels used in the best fit to the experimental data. Note that the acetylene rotational states are even/odd for dissociation from odd/even K_a' states. Individual dissociation probabilities are not given in this study since many of the peaks in the angular distributions result from the overlap of more than one channel. Particularly at larger angles, adjacent channels become highly correlated in such a way that the probability of an open channel can easily be transferred to another nearby channel without seriously compromising the quality of the fit. Therefore, only the relative probabilities for producing the various HCl j states are given in Table 1. Note that the results in parentheses for $j(\text{HCl}) = 3, 2, 1,$ and 0 are somewhat correlated so that really only their sum is meaningful. It is clear that the major channels correspond to the population of the C-C stretch of the acetylene fragment in combination with the highest possible $j(\text{HCl}) = 5$ and 6 , indicative of the inverted rotational distributions of the HCl fragment. From the quoted probabilities, we can derive that

TABLE 1: Probabilities and Energetics for the HCl Rotational States in the Photodissociation of Acetylene–HCl^a

$j(\text{HCl})$	$K_a = 2 \leftarrow 1$	$K_a = 0 \leftarrow 1$	$K_a = 1 \leftarrow 0$
6	0.18	0.11	0.19
5	0.36	0.42	0.42
4	0.16	0.13	0.18
3	(0.11)	(0.07)	(0.06)
2	(0.07)	(0.06)	(0.05)
1	(0.04)	(0.05)	(0.02)
0	(0.08)	(0.16)	(0.08)
average kinetic energy release	174	200	174
average vibrational energy in C ₂ H ₂ fragment	1974	1974	1974
average rotational energy in C ₂ H ₂ fragment	59	48	35
average rotational energy in HCl fragment	246	223	262

^a The individual probabilities for the lower $j(\text{HCl})$ states are placed in parentheses, as they are highly correlated and only their sum is meaningful. All quoted energies are in cm^{-1} .

(averaged over the three K_a sub-bands since there are no significant energetic differences) most of the available energy stays with the acetylene fragment in the form of vibration (81%, 1974 cm^{-1}) and rotation ($\approx 2\%$, 48 cm^{-1}), while only 10% (244 cm^{-1}) is found in the rotational degree of freedom of the HCl fragment, the remaining 7% (about 183 cm^{-1}) being in recoil kinetic energy.

As pointed out previously, there are other possible vibrational modes of the acetylene fragment that are nearly resonant in energy with the C–C stretch, namely the $2\nu_4 + \nu_5$ and $\nu_4 + 2\nu_5$. Dissociation into these channels seems unlikely, however, since a direct process would require high order coupling, owing to the large number of vibrational quantum numbers that would need to change.⁵

It is interesting to note that acetylene has a strong Fermi resonance between the (0010^00^0) state, normally pumped in these experiments, and the (0101^11^1) state. In the previous spectroscopic studies of both acetylene–HCl²² and acetylene–HF,⁴² we have shown that this Fermi resonance is significantly quenched by the complex formation, to the point where only one of the members of the diad has sufficient intensity to be observed experimentally. Nevertheless, this does not mean that the coupling is completely absent, to the point it does not influence the dissociation dynamics. In a number of previous studies, we have shown that this Fermi resonance can enhance the rate of dissociation.^{43,44} Since the C–C stretch (0100^00^0) is one of the modes associated with the dark state in this Fermi resonance and the two bending modes are of low enough frequency that the associated coupling could be quite large, it is reasonable to think about the dissociation proceeding most rapidly through the relaxation of these bends, resulting in the population of the C–C stretching state of the acetylene fragment.

As in our previous studies,^{38,40} we need to consider the possibility that the electric field influences the predissociation dynamics of the complex. First, we note that the interaction energy between the permanent electric dipole of the complex and the electric field is very small (of the order of 1 cm^{-1}) compared with the energies associated with the breaking of the intermolecular bond. The acetylene fragment has zero dipole moment, and the rotational constant of the HCl is so large that neither is significantly affected by the field. We can therefore

anticipate that the dissociation dynamics is relatively unaffected by the applied electric field. To test this, the probabilities obtained from the fit of the oriented $K_a = 1 \leftarrow 0$ angular distribution were used to calculate the angular distribution at zero electric field, resulting in the solid line shown in Figure 1. The agreement with experiment is clearly good, supporting our expectations.

In view of the results from the present study, we must reconsider our previous explanation for the excess line broadening observed in this complex. Indeed, the spectroscopic results indicate that the acetylene–HCl complex dissociated in 0.15–0.83 ns, depending irregularly on the individual j state of the complex, while acetylene–D³⁵Cl dissociation is much slower, namely 5.0 ns.²² The intermolecular V–V process (producing $\nu = 1$ HCl) suggested previously²² nicely explained this difference, given that it is nearly resonant in the former case and rather nonresonant in the latter. Although appealing, this explanation is inconsistent with the present data, forcing us to consider other possibilities. For example, consider the relative ability of the HCl and DCI fragments to carry away rotational energy. Indeed, production of the acetylene fragment in the C–C stretch excited state requires production of the HCl fragment in states up to $j = 6$ to conserve energy (see Figure 6). On the other hand, the smaller rotational constant associated with the DCI fragment requires that it be produced in even higher rotational states, namely up to $j = 8$. The population of these states requires high order terms in the anisotropy of the potential, making the dissociation more difficult. At the same time, the DCI will have smaller zero-point bending amplitude within the complex, due to its larger moment of inertia, making it even more closely “T-shaped” than the HCl complex, favoring the production of low j states. The combination of these two effects may be enough to account for the difference in the dissociation rates of the two isotopomers. What is still quite puzzling, however, is why acetylene–HCl dissociates much faster than acetylene–HF (3.6 ns^{42}), when the latter requires even lower rotational excitation ($j(\text{HF}) = 2$)³⁸ for the same channel. Nevertheless, this comparison is perhaps not as compelling given that the potential energy surfaces for these two systems are quite different. Indeed, the stronger intermolecular bonding in the acetylene–HF system, compared to acetylene–HCl, may result in an even weaker Fermi resonance for the former. Thus, if the Fermi resonance is the primary coupling responsible for the dissociation, the HF complex will have a longer lifetime than the corresponding HCl system.

It is now instructive to compare the dissociation energy obtained here ($D_0 = 830 \text{ cm}^{-1}$) with the results of a selected number of ab initio calculations. For example, Bacskay³³ has reported D_e values for this complex at both the MP2 and MP3 levels, yielding 3.01 kcal/mol (1053 cm^{-1}) and 2.57 kcal/mol (899 cm^{-1}), respectively. In this study, the zero-point energy was estimated using the harmonic frequencies, yielding $D_0 = 2.00 \text{ kcal/mol}$ (700 cm^{-1}). More recently, Araújo et al.³⁴ reported an MP2 value for D_e of 3.2 kcal/mol (1103 cm^{-1}). Similar calculations by Pople et al.²⁹ at the MP4 level yielded a D_0 of 1.9 kcal/mol (665 cm^{-1}). Since the anharmonic corrections to these zero-point energies will tend to increase these D_0 's, the agreement with the present experimental value is reasonable. All of these results clearly support the higher value for the dissociation energy obtained here, rather than the lower value ($170\text{--}260 \text{ cm}^{-1}$) reported previously.²³

Summary

In the present study, we have shown that the dissociation of acetylene proceeds via an intramolecular V–V process, produc-

ing acetylene in the C–C stretch excited state. The dissociation energy obtained from this study (830 cm^{-1}) is considerably larger than that reported previously,²³ but in reasonably good agreement with the best ab initio calculations.

A significant database is now becoming available from state-to-state photodissociation studies of weakly bound complexes, which includes final state distributions, dissociation energies, and dissociation rates. Although we are able to rationalize most of what we see and even make rough predictions for the rates,²⁰ we still have relatively little predictive capability concerning the state-to-state results. There is clearly much need for theoretical methods that can handle systems of this complexity, even though, with the number of open channels typical of these systems, they will necessarily need to be approximate. It is interesting to note that considerable progress has been made with exact methods on somewhat simpler systems, including diatom–diatom complexes such as HF dimer^{8,45} and $\text{D}_2\text{H}_2\text{--HF}$.^{7,46} The highly nonstatistical dissociation that is observed in these complexes promises many new insights into the detailed nature of vibrational dynamics, some of which is evident from the data itself. Nevertheless, to take full advantage of the information content in such experiments, we will need to make comparisons with the corresponding quantitative theories.

Acknowledgment. This work was supported by the National Science Foundation (CHE-97-10026). We also acknowledge the donors of the Petroleum Research Fund, administered by the ACS, for partial support of this research.

References and Notes

- (1) Miller, R. E. *Acc. Chem. Res.* **1990**, *23*, 10.
- (2) Nesbitt, D. J. *Annu. Rev. Phys. Chem.* **1994**, *45*, 367.
- (3) Zhao, Z.-Q.; Parmenter, C. S. *Ber. Bunsen-Ges. Phys. Chem.* **1995**, *99*, 536.
- (4) Hutson, J. M. *Annu. Rev. Phys. Chem.* **1990**, *41*, 123.
- (5) Ewing, G. E. *J. Phys. Chem.* **1987**, *91*, 4662.
- (6) Clary, D. C.; Knowles, P. J. *J. Chem. Phys.* **1990**, *93*, 6334.
- (7) Zhang, D. H.; Zhang, J. Z. H.; Bačić, Z. *J. Chem. Phys.* **1992**, *97*, 3149.
- (8) von Dirke, M.; Bačić, Z.; Zhang, D. H.; Zhang, J. Z. H. *J. Chem. Phys.* **1995**, *102*, 4382.
- (9) Le Roy, R. J.; Davies, M. R.; Lam, M. E. *J. Phys. Chem.* **1991**, *95*, 2167.
- (10) Villarreal, P.; Miret-Artés, S.; Roncero, O.; Delgado-Barrio, G.; Beswick, J. A.; Halberstadt, N.; Coalson, R. D. *J. Chem. Phys.* **1991**, *94*, 4230.
- (11) Huang, Z. S.; Jucks, K. W.; Miller, R. E. *J. Chem. Phys.* **1986**, *85*, 6905.
- (12) Block, P. A.; Miller, R. E. *Chem. Phys. Lett.* **1994**, *226*, 317.
- (13) Huang, Z. S.; Jucks, K. W.; Miller, R. E. *J. Chem. Phys.* **1986**, *85*, 3338.
- (14) Matsumoto, Y.; Ohshima, Y.; Takami, M. *J. Chem. Phys.* **1990**, *92*, 937.
- (15) Casassa, M. P.; Stephenson, J. C.; King, D. S. *J. Chem. Phys.* **1988**, *89*, 1966.
- (16) Beswick, J. A.; Jortner, J. *Chem. Phys. Lett.* **1977**, *49*, 13.
- (17) Beswick, J. A.; Jortner, J. *J. Chem. Phys.* **1978**, *68*, 2277.
- (18) Ewing, G. E. *J. Chem. Phys.* **1979**, *71*, 3143.
- (19) Ewing, G. E. *J. Chem. Phys.* **1980**, *72*, 2096.
- (20) Miller, R. E. *Science* **1988**, *240*, 447.
- (21) Legon, A. C.; Aldrich, P. D.; Flygare, W. H. *J. Chem. Phys.* **1981**, *75*, 625.
- (22) Dayton, D. C.; Block, P. A.; Miller, R. E. *J. Phys. Chem.* **1991**, *95*, 2881.
- (23) Rudich, Y.; Naaman, R. *J. Chem. Phys.* **1992**, *96*, 8616.
- (24) Gough, T. E.; Miller, R. E.; Scoles, G. *Appl. Phys. Lett.* **1977**, *30*, 338.
- (25) Loesch, H. J.; Remscheid, A. *J. Chem. Phys.* **1990**, *93*, 4779.
- (26) Friedrich, B.; Herschbach, D. R. *Nature (London)* **1991**, *353*, 412.
- (27) Friedrich, B.; Pullman, D. P.; Herschbach, D. R. *J. Phys. Chem.* **1991**, *95*, 8118.
- (28) Moore, D. T.; Oudejans, L.; Miller, R. E. *J. Chem. Phys.* **1999**, *110*, 197.
- (29) Pople, J. A.; Frisch, M. J.; Del Bene, J. E. *Chem. Phys. Lett.* **1982**, *91*, 185.
- (30) Hinchliffe, A. *Chem. Phys. Lett.* **1982**, *85*, 531.
- (31) De Almeida, W. B.; Hinchliffe, A. *Chem. Phys.* **1989**, *137*, 143.
- (32) Bacskay, G. B.; Kerdraon, D. I.; Hush, N. S. *Chem. Phys.* **1990**, *144*, 53.
- (33) Bacskay, G. B. *Mol. Phys.* **1992**, *77*, 61.
- (34) Araújo, R. C. M. U.; da Silva, J. B. P.; Ramos, M. N. *Spectrochim. Acta* **1995**, *51A*, 821.
- (35) Araújo, R. C. M. U.; Ramos, M. N. *J. Mol. Struct. (THEOCHEM)* **1996**, *366*, 233.
- (36) Bohac, E. J.; Marshall, M. D.; Miller, R. E. *J. Chem. Phys.* **1992**, *96*, 6681.
- (37) Oudejans, L.; Miller, R. E. *J. Phys. Chem.* **1995**, *99*, 13670.
- (38) Oudejans, L.; Moore, D. T.; Miller, R. E. *J. Chem. Phys.* **1999**, *110*, 209.
- (39) Bemish, R. J.; Bohac, E. J.; Wu, M.; Miller, R. E. *J. Chem. Phys.* **1994**, *101*, 9457.
- (40) Oudejans, L.; Miller, R. E. *J. Chem. Phys.* **1998**, *109*, 3474.
- (41) Oudejans, L.; Miller, R. E. *Chem. Phys.* **1998**, *239*, 345.
- (42) Huang, Z. S.; Miller, R. E. *J. Chem. Phys.* **1989**, *90*, 1478.
- (43) Bemish, R. J.; Miller, R. E. *Chem. Phys. Lett.* **1997**, *281*, 272.
- (44) Bemish, R. J.; Oudejans, L.; Miller, R. E.; Moszynski, R.; Heijmen, T. G. A.; Korona, T.; Wormer, P. E. S.; van der Avoird, A. *J. Chem. Phys.* **1998**, *109*, 8968.
- (45) Zhang, D. H.; Zhang, J. Z. H. *J. Chem. Phys.* **1993**, *99*, 6624.
- (46) Zhang, D. H.; Zhang, J. Z. H.; Bačić, Z. *J. Chem. Phys.* **1992**, *97*, 927.